Biointerface Research in Applied Chemistry
Platinum Open Access Journal (ISSN: 2069-5837)

Article
Volume 11, Issue 3, 2021, 9862 - 9870
https://doi.org/10.33263/BRIAC113.98629870

Enhanced Dielectric properties of Bismuth Doped Barium Titanate Ceramics with their Structural and Compositional Studies

Arijun Nahar [1,2], Mahabub Alam Bhuiyan [1,*], Mohammad Jellur Rahman [3], Shamima Choudhury [1]

[1] Department of Physics, University of Dhaka, Dhaka-1000, Bangladesh
[2] Materials Science Division, Bangladesh Atomic Energy Centre, Dhaka-1000, Bangladesh
[3] Department of Physics, Bangladesh University of Engineering and Technology (BUET), Dhaka-1000, Bangladesh
* Correspondence: mahabub@du.ac.bd;

Scopus Author ID 57213791571
Received: 1.09.2020; Revised: 18.09.2020; Accepted: 18.09.2020; Published: 22.09.2020

Abstract: Several strategies have been employed to tune the functional properties of environmentally friendly Barium titanate ($BaTiO_3$). In this work, bismuth (Bi) doped $BaTiO_3$ with a general formula $Ba_{1-x}Bi_{2x/3}TiO_3$ (where x = 0.00, 0.01, 0.02, 0.03, 0.04, 0.05 and 0.06) were prepared by the conventional solid-state reaction method. The effect of Bi on the structure of $BaTiO_3$; and their morphological and compositional studies were carried out by X-ray Diffraction (XRD), Scanning Electron Microscopy (SEM), and Energy Dispersive X-ray (EDX) respectively. Furthermore, the effect of Bi on the transport properties of $BaTiO_3$ was investigated. Our studies revealed that for x = 0.01, Bi doping gives rise to the highest tetragonality of the crystal with more homogeneous grains and pores distribution among all the doping concentration. Furthermore, the dielectric constant for x = 0.01 samples has been observed to be the highest, which is consistent with the structural and morphological studies. Also, the tetragonal to cubic phase transition temperature (Curie temperature) of the sample is found to increase with increasing Bi doping concentration. Our studies suggest that the higher value of the dielectric constant with higher Curie temperature can be obtained by a small amount of Bi doping (x = 0.01), which has potential applications in various electronic and energy storage devices.

Keywords: barium titanate; tetragonality; microstructure; dielectric constant; Curie temperature.

1. Introduction

Barium titanate ($BaTiO_3$) has been proven to be an excellent candidate as a ferroelectric ceramic [1]. The ferroelectricity of $BaTiO_3$ originates from the spontaneous polarization of the crystal below its transition temperature [2]. It has potential applications in various electronic devices as multilayer ceramic capacitors and positive temperature coefficient (PTC) resistors, ferroelectric memories, optoelectronic devices, piezoelectric sensors, energy storage systems, *etc.* [3-13] due to its large value of dielectric constant, very low dielectric loss, low leakage current and electro-optic coefficient [8, 9, 14-16]. Furthermore, various efforts such as microstructural and domain engineering, texturing, composite and core-shell approach, chemical doping have been employed to tune the functional properties of $BaTiO_3$ [12, 17-21]. Among those, chemical doping has become the most common and effective way to improve the transport and electrochemical properties of $BaTiO_3$ due to its reliable processing and low cost with large scalability [21].

In $BaTiO_3$ perovskite, the doping generally replaces either the A- or B- site cations depending on the valency and types of substituting ions [21]. Usually, a small amount of aliovalent or isovalent dopants are added prior to calcination, which can alter the properties of $BaTiO_3$ ceramic. Among a large number of available dopants, bismuth (Bi) has attracted the attention of many researchers due to its lone pair electrons ($6s^2$) and low sintering temperature [22-26]. This lone pair electron can cause the structural distortions as well as it can modify the crystallite size [27,28], and the low sintering temperature can reduce the energy consumption; thus, intriguing researchers to investigate the associated properties of the ceramic.

The effect of Bi on the structural, optical, ferroelectric, piezoelectric, and dielectric properties of $BaTiO_3$ have been recently studied by researchers for the samples synthesized by different methods such as the sol-gel method, water vapor atmosphere at elevated temperature, liquid state method, conventional solid-state reaction method, etc. [2, 21, 22, 29-32]. However, a few of those works have demonstrated very promising results, since the properties of the ceramic are very sensitive to many factors such as their preparation route, composition or chemical formula of the sample, sintering parameters, size of the crystallites, microstructure, etc. [4, 19, 21]. These open the door to explore and tailor the properties of this ceramic.

This present work demonstrates that a small amount of Bi doping in $BaTiO_3$ can change the tetragonality of the crystal structure, and a certain amount of this dopant concentration can improve the microstructure and enhance the transport properties of the prepared samples, which may have potential applications in electronic and energy storage devices.

2. Materials and Methods

The undoped $BaTiO_3$ and Bi-doped $BaTiO_3$ ceramics samples with the general formula $Ba_{1-x}Bi_{2x/3}TiO_3$ (where x = 0.00, 0.01, 0.02, 0.03, 0.04, 0.05 and 0.06) were prepared by the conventional solid-state reaction method. The high purity (>99%) raw barium carbonate ($BaCO_3$), titanium dioxide (TiO_2), and bismuth oxide (Bi_2O_3) powders (Merck, Darmstadt, Germany) were weighed appropriately according to the stoichiometric ratio to obtain the desired composition and then mixed thoroughly for 6 hours using agate and pestle to have a homogeneous mixture. The mixture was then dried, grounded for one hour, and calcined at 900 °C for 3 hours in a furnace (Type-ROS 3/20 FNR 7601905, Germany). Then the calcined powders were again dehand-milled for 2 hours, and a 5% polyvinyl alcohol solution was added as a binder. These hand-milled powders were then pressed to obtain tablet-shaped samples using a suitable die. Finally, the tablets were sintered at 1200 °C for 3 hours with a heating rate of 5 °C/minute and then cooled to room temperature (27 °C) with the same cooling rate. The sintered tablets were then polished and used for the structural, morphological, compositional, and transport measurements. The structural property was carried out by X-Ray Diffraction (XRD) using Philips X'pert PRO X-ray diffractometer (PW3040) with Cu-K_α radiation (λ = 1.5405 Å). The morphology, grain size, and compositional properties were investigated by a Hitachi S-3400N variable pressure Scanning Electron Microscope (SEM) equipped with an Energy Dispersive X-ray spectroscopy (EDX). For electrical measurements, the silver paste was used on both sides of the prepared tablets to have good electrical contact, and a Wayne Kerr 6500B series precision impedance analyzer was employed for the measurements.

3. Results and Discussion

From the XRD data (Figure 1), it is revealed that the diffraction peaks for (001), (101), (111), (002), (200), (210), (211), (202), and (003) planes match with the JCPDS 05-0626, which confirms that both the undoped and Bi-doped $BaTiO_3$ have single-phase tetragonal crystal structure with the space group *P4mm* [33]. Although the position of the peaks has not changed significantly with the increase in Bi content, after a certain amount of Bi content, the intensity of the (200) peak subsides. These indicate that the undoped and doped $BaTiO_3$ have almost the same structure, but the tetragonality (c/a) of the structure has been changed after a certain amount of Bi content [16]. We note that the acquired XRD data indicates the absence of any precursor phase of the raw materials.

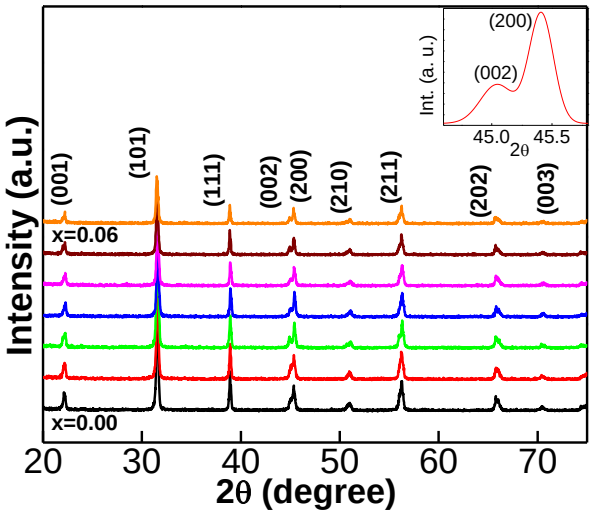

Figure 1. XRD pattern of $Ba_{1-x}Bi_{2x/3}TiO_3$ (where x = 0.00, 0.01, 0.02, 0.03, 0.04, 0.05 and 0.06). Inset shows the splitting of (002) and (200) peaks.

Table 1 shows the lattice parameter and tetragonality (c/a) of $Ba_{1-x}Bi_{2x/3}TiO_3$ ceramics. In determining the lattice parameters from the XRD data, the overlapped peaks (002) and (200) were enlarged and deconvoluted to avoid any possible error. The determined value of c/a (> 1.00) indicates the tetragonal phase of the prepared ceramics. From Table 1, it is noticed that the doping of $BaTiO_3$ with Bi changes the lattice parameter (c) of the unit cell and thus the tetragonality (c/a) of the crystal structure, which is notably the highest for x = 0.01 sample. These changes in the crystal structure may be attributed due to the substitution of trivalent Bi^{3+} ions into the Ba^{2+} site and the simultaneous reduction of oxygen vacancies. Furthermore, the lone pair electron of Bi^{3+} has a polarization effect on the off-centered Ti^{4+} ion, which might be responsible for this change in tetragonality [23].

Table 1. Lattice parameters (a and c), tetragonality (c/a) and grain size of the studied $Ba_{1-x}Bi_{2x/3}TiO_3$ (where x = 0.00 to 0.06) samples.

Bi Content (x)	Composite	Lattice parameters		Tetragonality (*c*/*a*)	Grain size (nm)
		a (Å)	*c* (Å)		
0.00	$BaTiO_3$	3.9793	4.0222	1.0108	168
0.01	$Ba_{0.99}Bi_{0.067}TiO_3$	3.9656	4.0389	1.0185	248
0.02	$Ba_{0.98}Bi_{0.013}TiO_3$	3.9716	4.0316	1.0151	340
0.03	$Ba_{0.97}Bi_{0.020}TiO_3$	3.9724	4.0357	1.0159	350
0.04	$Ba_{0.96}Bi_{0.026}TiO_3$	3.9836	4.0306	1.0118	370
0.05	$Ba_{0.95}Bi_{0.033}TiO_3$	3.9726	4.0321	1.0149	365
0.06	$Ba_{0.94}Bi_{0.040}TiO_3$	3.9753	4.0313	1.0141	534

Figure 2 shows the SEM images of the $Ba_{1-x}Bi_{2x/3}TiO_3$ (where x = 0.00 to 0.06) samples sintered at 1200 ℃ for 3 hours. From surface morphology of the undoped $BaTiO_3$ (x = 0.00), it is revealed that the grain size of the sample is very small (Table 1), density is poor, and it has the presence of porosity, but a small amount of Bi incorporation (x = 0.01) increases the grain size and density. Further increase in Bi doping (x = 0.02 to 0.06) also increases the grain size and density. However, a close examination of the microstructure images reveals that the grains and pores are homogeneous in size and they are more uniformly distributed for x = 0.01 compared to other Bi-doped samples (x = 0.02 to 0.06). For instance, in the SEM image of x = 0.03 sample, both small and large size grains, as well as randomly distributed inhomogeneous pores are easily manifested. This is attributed to the low solubility of Bi in $BaTiO_3$ [34]. The compositional study was carried out by the EDX detector, and an EDX spectrum as an example for x = 0.01 is presented in Figure 3. The EDX analysis confirmed the presence of Bi and that there is no impurity element in the prepared samples.

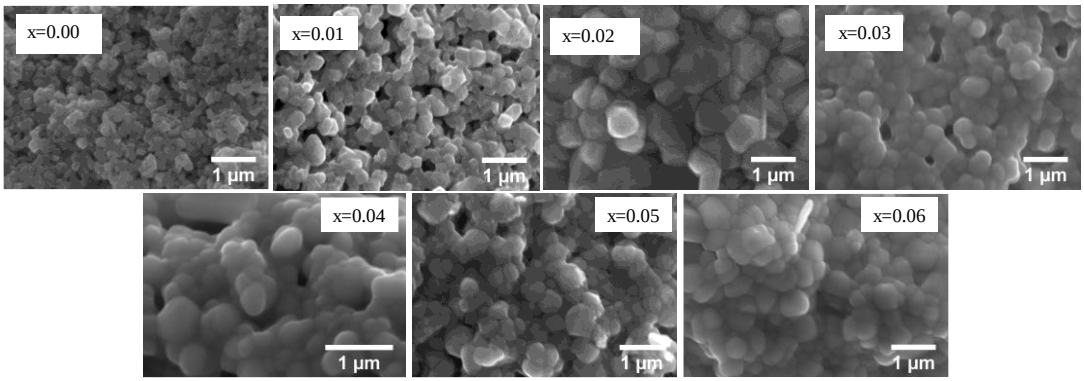

Figure 2. SEM images of $Ba_{1-x}Bi_{2x/3}TiO_3$ (x = 0.00, 0.01, 0.02, 0.03, 0.04, 0.05 and 0.06).

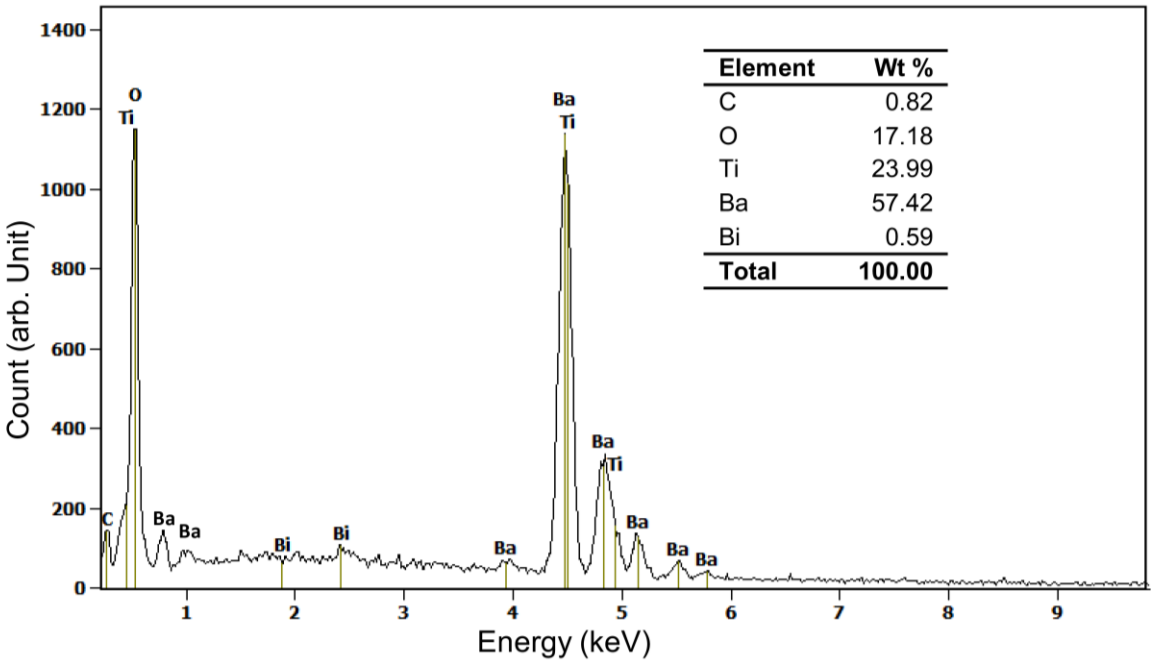

Figure 3. Typical EDX spectrum of $Ba_{1-x}Bi_{2x/3}TiO_3$ for x = 0.01. Inset shows the elemental data for that particular spectrum.

Figure 4(a) shows the frequency-dependent dielectric constant (ε_r) of the undoped and Bi incorporated $BaTiO_3$ ceramics sintered at 1200℃ for 3 hours, which was calculated by using the formula $\varepsilon_r = Cd/\varepsilon_0 A$, where d is the thickness of pellets, C is the capacitance, ε_0 is the

permittivity of free space, and *A* is the cross-sectional area of the pellets. The ε_r was measured in the frequency range 10^3 Hz to 10^6 Hz and observed to vary between 900 and 1900 depending on the amount of dopant. It is observed that the value of ε_r decreases very rapidly with the increase in frequency at the low-frequency range (<10^4 Hz), whereas it decreases very slowly at the high-frequency range, which is normal dielectric behavior of undoped and doped $BaTiO_3$ ceramics [9, 11, 35]. However, for x = 0.01 doped sample, the value of ε_r decreases a bit faster in the low-frequency range as compared to that of the undoped and other doped samples, as shown in figure 4(a). It can be considered that different kinds of polarization, such as dipolar, atomic, electronic, and interfacial polarization, are much more effective for this (x = 0.01) doped sample compared to other samples.

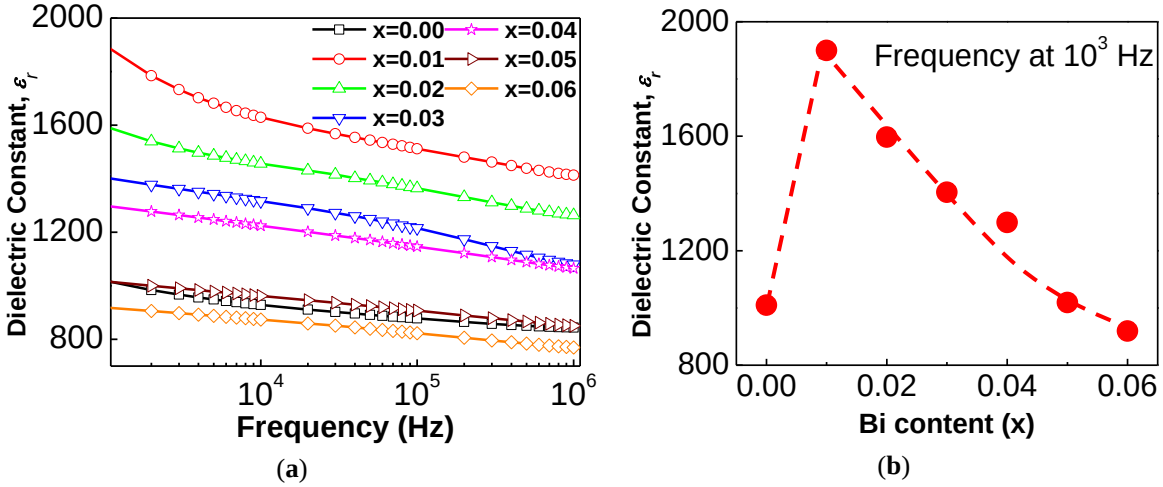

Figure 4. (a) Frequency-dependent dielectric constant and (b) Dielectric constant for different Bi doping concentration at frequency 10^3 Hz. The dashed line in (b) is a guide for the eyes.

The obtained room temperature ε_r values at 10^3 Hz for all the samples are plotted in Figure 4(b). These values indicate that a small amount of Bi (x = 0.01) doping gives the highest ε_r value, but a further increase of Bi in $Ba_{1-x}Bi_{2x/3}TiO_3$ reduces the ε_r value of the ceramic. Furthermore, the obtained value of ε_r at room temperature in our prepared sample for x = 0.01 is higher than the previously reported value of ε_r at room temperature for the Bi-doped $BaTiO_3$ ceramics synthesized by the same conventional solid-state reaction method [16, 30, 33]. This higher value of ε_r in our x = 0.01 Bi doping sample can be explained by the tetragonality (c/a) and microstructure of the prepared samples. The x = 0.01 Bi doping increases the lattice parameter (c), and thus, the tetragonality (c/a) of the crystal increases (as can be seen in Table 1). This creates a permanent electric dipole, which is responsible for a much higher value of ε_r. In addition to this tetragonality, the grain size and pores, and their even distribution throughout the sample in case of x = 0.01 Bi doping (Figure 2) with compared to undoped and other Bi-doped $BaTiO_3$ makes it possible to achieve the higher ε_r value. Further addition of Bi (x = 0.02 to 0.06) affects the lattice parameters of $BaTiO_3$ and thus decrease the tetragonality (c/a) of the structure as well as manifested inhomogeneity of the grain size and pores, and their uneven distribution reduces the value of ε_r.

Temperature-dependent DC electrical resistivity, ρ_{dc}, was measured for all $Ba_{1-x}Bi_{2x/3}TiO_3$ samples by using the formula $\rho_{dc} = \left(\frac{V_s}{V_F}\right)\left(\frac{A}{d}\right)R_F$, where *d* is the separation of the contacts, *A* is the cross-sectional area of the sample, V_s and V_F are the measured voltages across the sample and fixed resistance; and R_F is the standard fixed resistance. The measured values

are presented in Figure 5(a) as an Arrhenius plot (*lnρ vs. 1000/T*). It is observed that with the increase in temperature the ρ_{dc} the value passed through a sharp fall at a particular temperature and termed as Curie temperature, T_c, which indicates the tetragonal to cubic phase transition in $BaTiO_3$ samples [36]. It is noted that both undoped and doped samples exhibit a similar phase transition. However, the value of T_c is shifted linearly to the higher value with the increase in doping concentration in $BaTiO_3$, which can be seen in Figure 5(b). Here the lone pair effects of Bi^{3+} ion induces a local electric field, which then interacts with the ferroelectric unit cell and thereby increases the transition temperature [2].

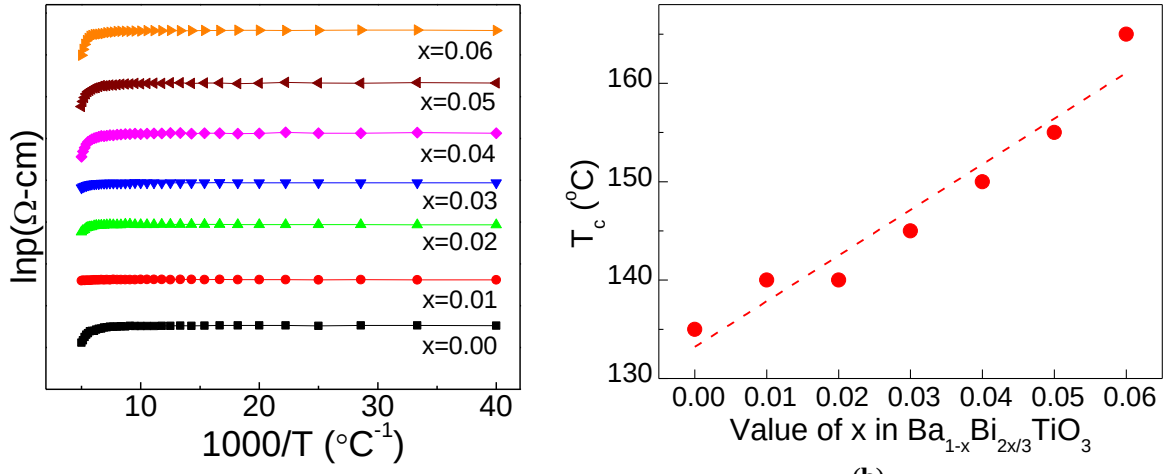

Figure 5. (a) lnρ vs 1⁄T plot for $Ba_{1-x}Bi_{2x/3}TiO_3$ (x=0.00, 0.01, 0.02, 0.03, 0.04, 0.05 and 0.06) ceramics. (b) Doping concentration-dependent transition temperature. The line is a guide for the eyes.

DC electrical resistivity for all the samples both at room temperature and at the transition temperature are presented in Table 2. Here, it is observed that the resistivity at these temperatures followed an almost decreasing trend with increasing the doping concentration. This may be attributed to the increase in the grain size of the specimen and the high concentration of free carriers [37].

Table 2. DC electrical resistivity at room temperature and at the transition temperature for $Ba_{1-x}Bi_{2x/3}TiO_3$ (x = 0.00, 0.01, 0.02, 0.03, 0.04, 0.05 and 0.06) ceramics.

Value of x in $Ba_{1-x}Bi_{2x/3}TiO_3$	ρ_{dc} at room temperature (10^7 Ω-cm)	ρ_{dc} at T_c (10^7 Ω-cm)
0.00	2.143	2.130
0.01	2.088	2.090
0.02	2.150	2.150
0.03	2.047	2.042
0.04	1.839	1.831
0.05	1.670	1.635
0.06	1.874	1.826

4. Conclusions

Bi-doped $BaTiO_3$ ceramic with the general formula $Ba_{1-x}Bi_{2x/3}TiO_3$ (where x = 0.00, 0.01, 0.02, 0.03, 0.04, 0.05 and 0.06) were prepared by the conventional solid-state reaction method. The structural, compositional, and morphological studies were carried out by XRD, EDX, and SEM. Our studies showed that a small amount of Bi doping (x = 0.01) increases the tetragonality of the crystal and can improve the microstructure of the specimen, but further doping concentration (x > 0.01) decreases the tetragonality as well as degrade the microstructure of the ceramic. The studies of transport properties revealed that this small

amount of Bi-doped (x = 0.01) $BaTiO_3$ sample achieve the highest value of room-temperature dielectric constant at 1.0 kHz with higher Curie temperature, which is higher than the previously reported value for Bi-doped $BaTiO_3$ sample prepared by the same route. These were achieved due to the higher tetragonality of the structure and better compaction of the prepared sample with more homogeneous grain growth. Thus, the incorporation of an appropriate amount of Bi can be employed to obtain enhanced properties of $BaTiO_3$ for various electronic and energy storage applications. Furthermore, our findings will stimulate many researchers to exploit the influence of Bi doping in $BaTiO_3$ ceramics and thus will enrich the current library of ferroelectric materials.

Funding

This research received no external funding.

Acknowledgments

The authors are grateful to the research facilities of Nano and Advanced Materials Lab, Department of Physics, University of Dhaka; Department of Physics, Bangladesh University of Engineering and Technology (BUET); Materials Science Division, Bangladesh Atomic Energy Centre (BAEC), Dhaka; and Industrial Physics Division, BCSIR, Dhaka.

Conflicts of Interest

The authors declare no conflict of interest.

References

1. Akbarian, D.; Yilmaz, D.E.; Cao, Y.; Ganesh, P.; Dabo, I.; Munro, J.; Ginhovend, R.V.; van Duin, A.C.T. Understanding the influence of defects and surface chemistry on ferroelectric switching: a ReaxFF investigation of $BaTiO_3$. *Phys. Chem. Chem. Phys.* **2019**, *21*, 18240-18249, https://doi.org/10.1039/C9CP02955A.
2. Kholodkova, A.; Smirnov, A.; Danchevskaya, M.; Ivakin, Y.; Muravieva, G.; Ponomarev, S.; Fionov, A.; Kolesov, V. Bi_2O_3-Modified Ceramics Based on $BaTiO_3$ Powder Synthesized in Water Vapor. *Inorganics* **2020**, *8*, https://doi.org/10.3390/inorganics8020008.
3. Hong, K.; Lee, T.H.; Suh, J.M.; Yoon, S.-H.; Jang, H.W. Perspectives and challenges in multilayer ceramic capacitors for next generation electronics. *J. Mater. Chem. C* **2019**, *7*, 9782-9802, https://doi.org/10.1039/C9TC02921D.
4. Yoon, S.H.; Kima, M.Y.; Kim, D. Correlation between tetragonality (c/a) and direct current (dc) bias characteristics of $BaTiO_3$-based multilayer ceramic capacitors (MLCC). *J. Mater. Chem. C* **2020**, *8*, 9373-9381, https://doi.org/10.1039/D0TC02067B.
5. Yao, F.Z.; Yuan, O.; Wang, Q.; Wang, H. Multiscale structural engineering of dielectric ceramics for energy storage applications: from bulk to thin films. *Nanoscale* **2020**, *12*, 17165-17184, https://doi.org/10.1039/D0NR04479B.
6. Huybrechts, B.; Ishizaki, K.; Takata, M. The positive temperature coefficient of resistivity in barium titanate. *J. Mater. Sci.* **1995**, *30*, 2463–2474, https://doi.org/10.1007/BF00362121.
7. Brutchey, R.L.; Cheng, G.S.; Gu, Q.; Morse, D.E. Positive Temperature Coefficient of Resistivity in Donor-Doped $BaTiO_3$ Ceramics derived from Nanocrystals synthesized at Low Temperature. *Adv. Mater.* **2008**, *20*, 1029–1033, https://doi.org/10.1002/adma.200701804.
8. Vijatovic, M.M.; Bobic, J.D.; Stojanovc, B.D. History and challenges of barium titanate: Part I. *Sci. Sinter.* **2008**, *40*, 155–165, https://doi.org/10.2298/SOS0802155V.
9. Yasmin, S.; Choudhury, S.; Hakim, M.A.; Bhuiyan, A.H.; Rahman, M.J. Effect of Cerium Doping on Microstructure and Dielectric Properties of $BaTiO_3$ Ceramics. *J. Mater. Sci. Technol.* **2011**, *27*, 759–763, https://doi.org/10.1016/S1005-0302(11)60139-4.
10. Li, W.B.; Zhou, D.; He, B.; Li, F.; Pang, L.-X.; Lu, S.-G. Structure and dielectric properties of $Nd(Zn_{1/2}Ti_{1/2})O_3$ –$BaTiO_3$ ceramics for energy storage applications. *J. Alloys Comp.* **2016**, *685*, 418–422, https://doi.org/10.1016/j.jallcom.2016.05.311.

11. Mostafa, M.; Rahman, M.J.; Choudhury, S. Enhanced dielectric properties of $BaTiO_3$ ceramics with cerium doping, manganese doping and Ce-Mn co-doping. *Sci. Eng. Compos. Mater.* **2019**, *26*, 62–69, https://doi.org/10.1515/secm-2017-0177.
12. Gao, J.; Xue, D.; Liu, W.; Zhou, C.; Ren, X. Recent Progress on $BaTiO_3$-Based Piezoelectric Ceramics for Actuator Applications. *Actuators* **2017**, *6*, https://doi.org/10.3390/act6030024.
13. Somiya, S.; Komarneni, S.; Roy, R. Ceramic Powders for Advanced Ceramics: What are Ideal Ceramic Powders for Advanced Ceramics? *Trans. Mater. Res. Soc. Japan* **2010**, *35*, 473–483, https://doi.org/10.14723/tmrsj.35.473.
14. Luo, H.; Zhou, X.; Ellingford, C.; Zhang, Y.; Chen, S.; Zhou, K.; Zhang, D.; Bowen, C. R.; Wan, C. Interface design for high energy density polymer nanocomposites. *Chem. Soc. Rev.* **2019**, *48*, 4424-4465, https://doi.org/10.1039/C9CS00043G.
15. Sada, T.; Tsuji, K.; Ndayishimiye, A.; Fan, Z.; Fujioka, Y.; Randall, C.A. High permittivity $BaTiO_3$ and $BaTiO_3$-polymer nanocomposites enabled by cold sintering with a new transient chemistry: $Ba(OH)_2{\cdot}8H_2O$. *J. Eur. Ceram. Soc.* **2020**, in press, https://doi.org/10.1016/j.jeurceramsoc.2020.07.070.
16. Maurya, D.; Priya, S. Effect of Bismuth Doping on the Dielectric and Piezoelectric Properties of $Ba_{1-x}Bi_xTiO_3$ Lead-Free Ceramics. *Integr. Ferroelectr.* **2015**, *166*, 186–196, https://doi.org/10.1080/10584587.2015.1092629.
17. Jones, J.L.; Iverson, B.J.; Bowman, K.J. Texture and Anisotropy of Polycrystalline Piezoelectrics. *J. Am. Ceram. Soc.* **2007**, *90*, 2297–2314, https://doi.org/10.1111/J.1551-2916.2007.01820.X.
18. Takahashi, H. Development of lead-free $BaTiO_3$ ceramics possessing enhanced piezoelectric properties. *Electron. Commun. Jpn.* **2012**, *95*, 20–26, https://doi.org/10.1002/ecj.10418.
19. Zheng, P.; Zhang, J.L.; Tan, Y.Q.; Wang, C.L. Grain-size effects on dielectric and piezoelectric properties of poled $BaTiO_3$ ceramics. *Acta Mater.* **2012**, *60*, 5022–5030, https://doi.org/10.1016/j.actamat.2012.06.015.
20. Groh, C.; Franzbach, D.J.; Jo, W.; Webber, K.G.; Kling, J.; Schmitt, L.A.; Kleebe, H.-J.; Jeong, S.-J.; Lee, L.-S.; Rodel, J. Relaxor/Ferroelectric Composites: A Solution in the Quest for Practically Viable Lead-Free Incipient Piezoceramics. *Adv. Funct. Mater.* **2014**, *24*, 356–362, https://doi.org/10.1002/adfm.201302102.
21. Acosta, M.; Novak, N.; Rojas, V.; Patel, S.; Vaish, R.; Koruza, J.; Rossetti, G.A.; Rödel, J. $BaTiO_3$-based piezoelectrics: Fundamentals, current status, and perspectives. *Appl. Phys. Rev.* **2017**, *4*, 041305, https://doi.org/10.1063/1.4990046.
22. Jiang, X.P.; Zeng, M.; Kowk, K.W.; Chan, H.L.W. Dielectric and ferroelectric properties of Bi-doped $BaTiO_3$ ceramics. *Key Eng. Mater.* **2007**, *334-335*, 977-980, https://doi.org/10.4028/www.scientific.net/KEM.334-335.977.
23. Mahajan, S.; Thakur, O.P.; Bhattacharya, D.K.; Sreenivas, K. Ferroelectric relaxor behaviour and impedance spectroscopy of Bi_2O_3-doped barium zirconium titanate ceramics. *J. Phys. D: Appl. Phys.* **2009**, *42*. https://doi.org/10.1088/0022-3727/42/6/065413.
24. Nath, A.K.; Medhi, N. Piezoelectric properties of environmental friendly bismuth doped barium titanate ceramics. *Mater. Lett.* **2012**, *73*, 75-77, https://doi.org/10.1016/j.matlet.2011.12.113.
25. Wu, S.; Wei, X.; Wang, X.; Yang, H.; Gao, S. Effect of Bi_2O_3 Additive on the Microstructure and Dielectric Properties of $BaTiO_3$-Based Ceramics Sintered at Lower Temperature. *J. Mater. Sci. Technol.* **2010**, *26*, 472–476, https://doi.org/10.1016/S1005-0302(10)60075-8.
26. Vittayakorn, W.C.; Banjong, D.; Vittayakorn, N. Processing and Characterization of Bi_2O_3/$BaTiO_3$ Ceramic. *Adv. Mater. Res.* **2013**, *802*, 7-11, https://doi.org/10.4028/www.scientific.net/AMR.802.7.
27. Seshadri, R.; Hill, N.A. Visualizing the Role of Bi 6s "Lone Pairs" in the Off-Center Distortion in Ferromagnetic $BiMnO_3$. *Chem. Mater.* **2001**, *13*, 2892–2899, https://doi.org/10.1021/cm010090m.
28. Keeble, D.S.; Barney, E.R.; Keen, D.A.; Tucker, M.G.; Kreisel, J.; Thomas, P.A. Bifurcated Polarization Rotation in Bismuth-Based Piezoelectrics. *Adv. Funct. Mater.* **2013**, *23*, 185–190, https://doi.org/10.1002/adfm.201201564.
29. Attar, A.S.; Sichani, E.S.; Sharafi, S. Structural and dielectric properties of Bi-doped barium strontium titanate nanopowders synthesized by sol-gel method. *J. Mater. Res. Technol.* **2017**, *6*, 108–115, https://doi.org/10.1016/j.jmrt.2016.05.001.
30. Mahapatra, A.; Parida, S.; Sarangi, S.; Badapanda, T. Dielectric and Ferroelectric Behavior of Bismuth-Doped Barium Titanate Ceramic Prepared by Microwave Sintering. *JOM* **2015**, *67*, 1896–1904, https://doi.org/10.1007/s11837-014-1266-7.
31. Wang, J.; Rong, G; Li, N.; Li, C.; Jiang, Q.; Cheng, H. Dielectric Properties of Bi-Doped $BaTiO_3$-Based Ceramics Synthesized by Liquid-State Method. Russ. *J. Appl. Chem.* **2015**, *88*, 533−537, https://doi.org/10.1134/S107042721503026X.
32. Sareecha, N.; Shah, W.A.; Mirza, M.L.; Maqsood, A.; Awan, M.S. Electrical investigations of Bi-doped $BaTiO_3$ ceramics as a function of temperature. *Physica B: Condensed Matter* **2018**, *530*, 283-289, https://doi.org/10.1016/j.physb.2017.11.069.
33. Badapanda, T.; Senthil, V.; Rana, D.K.; Panigrahi, S.; Anwar, S. Relaxor ferroelectric behavior of "A" site deficient Bismuth doped Barium Titanate ceramic. *J. Electroceram.* **2012**, *29*, 117–124, https://doi.org/10.1007/s10832-012-9754-z.

34. Zhou, L.; Vilarinho, P.M.; Baptista, J.L.Solubility of bismuth oxide in barium titanate. *J. Am. Ceram. Soc.* **1999**, *82*, 1064–66, https://doi.org/10.1111/j.1151-2916.1999.tb01875.x.
35. Sen, S.; Choudhary, R.N.P. Structural, dielectric and electrical properties of Ca modified $BaSn_{0.15}Ti_{0.85}O_3$ ceramics. *J. Mater. Sci.* **2005**, *40*, 5457–5462, https://doi.org/10.1007/S10853-005-1908-9.
36. Merz, W.J. Double hysteresis loop of $BaTiO_3$ at the Curie point. *Phys. Rev.* **1953**, *91*, https://doi.org/10.1103/PhysRev.91.513.
37. Petrovic, M.M.V.; Bobic, J.D.; Ramoska, T.; Banys, J.; Stojanovic, B.D. Antimony doping effect on barium titanate structure and electrical properties. *Ceram. Int.* **2011**, *37*, 2669–2677, https://doi.org/10.1016/j.ceramint.2011.04.015.